A human promyelocytic-like population is responsible for the immune suppression mediated by myeloid-derived suppressor cells

Samantha Solito,[1] Erika Falisi,[1] Claudia Marcela Diaz-Montero,[2] Andrea Doni,[3] Laura Pinton,[1] Antonio Rosato,[1-4] Samuela Francescato,[5] Giuseppe Basso,[5] Paola Zanovello,[1-4] Georgiana Onicescu,[6] Elizabeth Garrett-Mayer,[6] Alberto J. Montero,[2] Vincenzo Bronte,[4] and Susanna Mandruzzato[1-4]

[1]Department of Oncology and Surgical Sciences, Oncology Section, University of Padova, Padova, Italy; [2]Department of Medicine, Sylvester Comprehensive Cancer Center, University of Miami, Miami, FL; [3]Laboratory of Immunology and Inflammation, Istituto Clinico Humanitas, Istituto Di Ricovero e Cura a Carattere Scientifico (IRCCS), Rozzano, Milan, Italy; [4]Istituto Oncologico Veneto IOV-IRCCS, Padova, Italy; [5]Laboratory of Oncohematology, Department of Pediatrics, University of Padova, Padova, Italy; and [6]Department of Medicine and Division of Biostatistics and Epidemiology, Medical University of South Carolina Hollings Cancer Center, Charleston, SC

We recently demonstrated that human BM cells can be treated in vitro with defined growth factors to induce the rapid generation of myeloid-derived suppressor cells (MDSCs), hereafter defined as BM-MDSCs. Indeed, combination of G-CSF + GM-CSF led to the development of a heterogeneous mixture of immature myeloid cells ranging from myeloblasts to band cells that were able to suppress alloantigen- and mitogen-stimulated T lymphocytes. Here, we further investigate the mechanism of suppression and define the cell subset that is fully responsible for BM-MDSC–mediated immune suppression. This population, which displays the structure and markers of promyelocytes, is however distinct from physiologic promyelocytes that, instead, are devoid of immuosuppressive function. In addition, we demonstrate that promyelocyte-like cells proliferate in the presence of activated lymphocytes and that, when these cells exert suppressive activity, they do not differentiate but rather maintain their immature phenotype. Finally, we show that promyelocyte-like BM-MDSCs are equivalent to MDSCs present in the blood of patients with breast cancer and patients with colorectal cancer and that increased circulating levels of these immunosuppressive myeloid cells correlate with worse prognosis and radiographic progression. (*Blood*. 2011;118(8): 2254-2265)

Introduction

One of the mechanisms of immune tolerance induced by cancer is based on the expansion of myeloid-derived suppressor cells (MDSCs), a heterogeneous population of immature myeloid cells, which accumulate in the blood, lymph nodes, BM, and tumor sites in patients and experimental animals with neoplasia, capable of inhibiting both adaptive and innate immunities.[1,2] The heterogeneity of MDSCs has always been a hallmark of this cell population since its original description, and many studies advanced that MDSCs might be composed of cells at several stages of differentiation of the myeloid lineage (Lin) sharing the same functional properties.[2] To explain this heterogeneity, it was advanced that the patterns of cytokines/chemokines that arm myeloid cells with inhibitory function may be tumor dependent. For all these reasons, MDSCs have been shown to express different surface markers, depending both on the stage of myeloid development examined and the differentiation context provided by factors secreted by cancer cells.

In this respect, we recently demonstrated that the cytokines GM-CSF, G-CSF, and IL-6 allowed a rapid generation of MDSCs from precursors present in human BM and that the immunoregulatory activity of BM-derived MDSCs (BM-MDSCs) depended on the C/EBPβ transcription factor.[3]

In the present study, we further characterized BM-MDSC mediated-immune suppression. Analogously to tumor-induced MDSCs, BM-MDSCs consist of a heterogeneous population of immature myeloid cells. We thus investigated whether the immune regulatory function of BM-MDSCs could be attributed to different myeloid subsets induced by cytokine treatment or rather to a specific subpopulation. Our results indicate that only one immature cell population, with structure and phenotype resembling promyelocytes, is responsible for the whole immune suppression mediated by BM-MDSCs and that a cell population with a similar phenotype is expanded in patients with breast cancer and patients with colorectal cancer.

Methods

BM samples, human cohorts, and treatments

Fresh BM aspirate samples with normal cytologic characteristics were obtained from patients enrolled in the protocol AIEOP-BFM-ALL 2000, with suspected leukemia or lymphomas, patients with lymphatic leukemia after 78 days without recurrences, and patients with lymphatic leukemia after BM transplantation as a part of the diagnostic follow-up. Informed consent was obtained from all participating persons, in compliance with the Declaration of Helsinki, before the study that was approved by the ethics committee of the Azienda Ospedaliera of Padova. For more details, see supplemental Methods (available on the *Blood* Web site; see the Supplemental Materials link at the top of the online article).

Submitted December 20, 2010; accepted June 21, 2011. Prepublished online as *Blood* First Edition paper, July 6, 2011; DOI 10.1182/blood-2010-12-325753.

The online version of this article contains a data supplement.

The publication costs of this article were defrayed in part by page charge payment. Therefore, and solely to indicate this fact, this article is hereby marked "advertisement" in accordance with 18 USC section 1734.

BM aspirates were subjected to lysis to remove red blood cells, with a hypotonic solution of ammonium chloride. Cells were plated (2×10^6 cells/well) into a 24-well tissue culture plate (Becton Dickinson) in IMDM (Gibco Invitrogen) supplemented with 10% FBS (Gibco), 0.01M HEPES, penicillin/streptomycin, and β-mercaptoethanol. Cells were cultured with 40 ng/mL G-CSF and GM-CSF for 4 days at 37°C, 8% CO_2. Human recombinant GM-CSF was a gift from J. F. Parkinson (Bayer Healthcare Pharmaceuticals), human recombinant G-CSF was purchased from Sanofi Aventis.

Patients with solid tumors

Peripheral blood specimens were collected from patients with stage IV colorectal cancer (n = 25) at the University of Miami Sylvester Comprehensive Cancer Center (UMSCCC) and stage IV breast cancer (n = 25) at UMSCCC and at the Medical University of South Carolina Hollings Cancer Center starting a new line of therapy. Venous blood was collected in K2 EDTA lavender-topped tubes (BD) before initiation of therapy, after every other cycle of therapy, and at the time of progression. Protocol Review Committees at Hollings Cancer Center and UMSCCC and Institutional Review Boards at both institutions approved this study. Written consent was obtained from all subjects.

Patients with solid tumors: statistical

Random effects linear regression was used to model the association between MDSCs and time in responders and nonresponders. The outcome was log (MDSCs), and predictors were time, response status, and an interaction between time and response. Random intercepts were included to account for correlation of repeated measures of MDSCs over time from the same patients. The coefficient on the interaction term was tested to determine whether the change in MDSCs over time was the same compared with difference in responders and nonresponders whereby an α level of 0.05 was used. Results were displayed graphically whereby each patient's MDSC responses are shown over time, with the estimated regression model shown as solid straight lines. Standard model diagnostics were used to ensure that assumptions about residuals were met. Kaplan-Meier analysis was used to estimate survival distributions, and differences in survival were tested with log-rank tests. Linear regression was used to determine association between circulating tumor cells (CTCs), Swenerton score (SS), and MDSCs, including estimation of slope, correlation coefficient, and statistical significance of the association. Overall survival (OS) was defined as time of study enrollment to date of death.

Flow cytometric analysis, Abs, and reagents

Cells were harvested and incubated with FcReceptor (FcR) Blocking Reagent (Miltenyi Biotec) to saturate FcR and then labeled with monoclonal Abs. For a detailed description of the Abs and of the methods used for labeling, see supplemental Methods. Data acquisition was performed with FACSCalibur or LSRII flow cytometer (Becton Dickinson), and data were analyzed with FlowJo software (TreeStar Inc).

Cytospin preparation

Cytospins were obtained by centrifuging 1×10^4 cells on microscope slides and stained with May-Grünwald-Giemsa dye (Bio-Optica) for 5 and 15 minutes, respectively. Cell morphology was examined by microscopic evaluation of stained cells using a Leica DM 2000 microscope (Leica Microsystems) with Leica lenses at 40× magnification and without immersion oil. Pictures were taken using a Leica DFC 295 camera (Vashaw Scientific Inc), acquired with Leica Acquisition Suite Version 3.5 (Meyer Instruments) and processed with Adobe Photoshop CSI (Adobe Systems).

Confocal microscopic analysis

Cells were fixed with 4% paraformaldehyde on polylysinated 14-mm round Menzel-Glaser glass in the dark for 15 minutes at room temperature and permeabilized for 5 minutes with 0.1% Triton X-100 (Sigma-Aldrich) in PBS, pH 7.4, before incubation for 1 hour at room temperature with PBS 2% BSA (Sigma-Aldrich) and 5% normal goat serum (Sigma-Aldrich). Cells were stained with mAb diluted in PBS 0.5% Tween for 1 hour at room temperature in the dark. Slides were then washed with the same buffer and incubated with the secondary Abs for 1 hour at room temperature in the dark. For a detailed description of the Abs and of the methods used for confocal microscopy, see supplemental Methods.

Separation of BM-MDSC subsets

Lin^- and Lin^+ fractions were separated from BM-MDSCs with Lineage Cell Depletion Kit (Miltenyi Biotec), a magnetic labeling system for the depletion of mature hematopoietic cells, following the manufacturer's instructions.

Myeloid fractions were also separated through cell sorting. Briefly, single-cell suspensions of ex vivo BM or BM-MDSCs were stained with anti-CD11b–PE, anti-CD16–FITC, and anti-CD3ϵ–PC7 and sorted on a MoFlo (DakoCytomation). $CD11b^{low/-}/CD16^-$ cells, $CD11b^+/CD16^-$ cells, and $CD11b^+/CD16^+$ cells were isolated, excluding lymphocytes, on the basis of CD3 expression and forward/side scatter parameters. All the fractions were obtained with a purity of ≥ 90%. Alternatively, myeloid populations were isolated through 2 consecutive magnetic sortings; in the first round, BM-MDSCs were depleted of $CD3\epsilon^+/CD19^+/CD56^+$ lymphocytes, with a cocktail of immunomagnetic beads obtained by combining anti–human CD3ϵ, CD19, and CD56 beads (Miltenyi Biotec). Subsequently, the $CD3\epsilon^-/CD19^-/CD56^-$ fraction was depleted of $CD11b^+$ cells with immunomagnetic anti–human CD11b beads (Miltenyi Biotec).

CFSE or CellTrace labeling and proliferation assay

PBMCs were isolated from the peripheral blood of healthy donors by density centrifugation as described.[4] Cell purity was checked by FACS analysis on forward/side scatter parameters, and viability was checked by Trypan blue dye exclusion.

PBMCs were stained with CFSE (Invitrogen Molecular Probe; range, 2-4μM) or with 2μM CellTrace Violet Cell Proliferation Kit (Invitrogen Molecular Probe), according to the manufacturer's instructions. For a detailed description of the methods of the labeling and proliferation assay, see supplemental Methods.

Isolation of human monocytes and granulocytes

Human granulocytes and PBMCs used for confocal microscopic analysis were obtained from peripheral blood of healthy donors, as described,[4] whereas human monocytes were prepared from PBMCs by short-term adherence to plastic. Briefly, PBMCs were isolated from leukocyte-enriched buffy coats (Transfusion Center) and incubated for 1 hour at 37°C and 5% CO_2 in flasks (Becton Dickinson) with the use of RPMI 1640 medium (Life Technologies) supplemented with 3% human serum. Nonadherent cells were removed by washing gently the flask with RPMI 1640 medium, and adherent monocytes were removed for successive analysis.

Statistical analysis

The statistical significance to compare parametric groups was determined by the Student *t* test, whereas the Mann-Whitney *U* test was used to compare nonparametric groups. Values were considered statistically significant with $P < .05$. Absence of significance was not reported for brevity.

Results

BM-MDSCs down-regulate the CD3ζ chain expression in $CD8^+$ T cells and require a cell-to-cell contact to inhibit alloantigen-activated T lymphocytes

BM-MDSCs consist of a heterogeneous combination of immature myeloid cells that, based on the combined staining with anti-CD11b and anti-CD16 Abs, can be qualified as differentiating cells that range from myeloblasts to band cells, albeit with variable

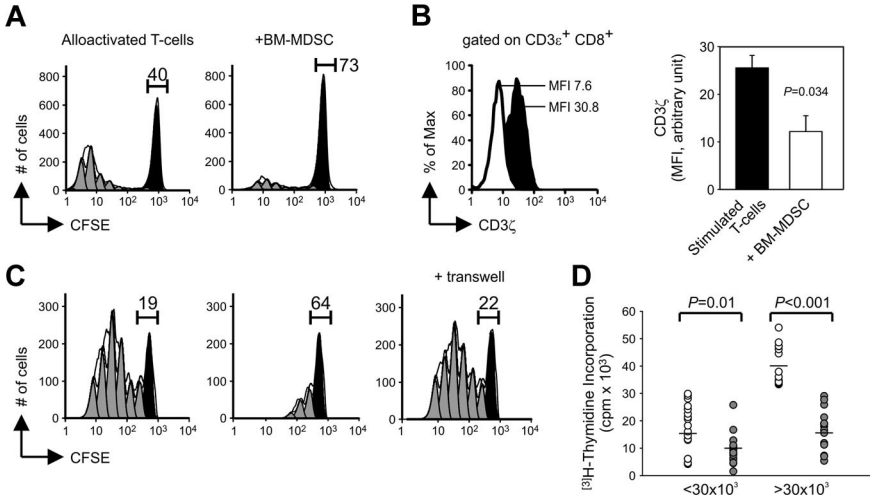

Figure 1. Characterization of BM-MDSC–mediated immune suppression. (A) CFSE-labeled PBMCs were stimulated with allogeneic γ-irradiated PBMCs without (left) or with (right) γ-irradiated BM-MDSCs added at a ratio of 1:1. After 7 days, cell cultures were harvested, labeled with anti-CD3ϵ, and analyzed in the $CD3\epsilon^+/CFSE^+$ cell gate. The figure shows a representative experiment of cell division analysis of 3 performed. The percentages of the undivided cells are indicated. (B) After 7 days of culture, cultures set up as in panel A were labeled with anti-CD3ϵ, anti-CD8, fixed, and then labeled with anti-CD3ζ. Mean fluorescence intensity (MFI) of CD3ζ was calculated in the $CFSE^+/CD3\epsilon^+/CD8^+$ cell gate. On the left panel, black histogram represents the MFI of stimulated PBMCs without BM-MDSCs, whereas the white histogram refers to MFI of stimulated PBMCs in presence of γ-irradiated BM-MDSCs. On the right panel, MFI values of CD3ζ are presented as mean ± SE of 3 independent experiments; $P = .034$, Student *t* test. (C) PBMCs were labeled with CFSE and stimulated with coated anti-CD3 and soluble anti-CD28 (left) and cocultured with BM-MDSCs in the presence (right) or in the absence (center) of a transwell. After 4 days, cells were harvested, labeled with anti-CD3ϵ, and analyzed in the $CD3\epsilon^+/CFSE^+$ gate. The figure shows a representative experiment of 3. The percentages of the undivided cells are indicated. (D) Proliferation of alloactivated PBMCs cocultured either with or without γ-irradiated BM-MDSCs was assessed by ^{3}H-thymidine incorporation. White dots represent the proliferation of stimulated PBMCs without BM-MDSCs, and gray dots correspond to the proliferation of alloactivated PBMCs in presence of BM-MDSCs. Twenty independent experiments are shown with proliferation of alloactivated PBMCs $< 30 \times 10^3$ cpm (columns 1 and 2) and 15 experiments with proliferation $> 30 \times 10^3$ cpm (columns 3 and 4). $P = .01$ and $P < .001$, Mann-Whitney *U* test.

proportions in different cultures.[3] We initially addressed whether some of MDSC functional properties, described both in mice and patients with cancer, were also shared by BM-MDSCs. In this regard, one of the mechanisms proposed to explain T-cell dysfunction induced by MDSCs is the proliferative arrest of Ag-activated T cells caused by loss of CD3ζ chain expression,[5] a proximal TCR-associated signaling molecule necessary for correct assembly and function of the TCR itself.

To understand whether BM-MDSC–mediated immune suppression induced a decrease in CD3ζ expression, we set up allogeneic MLRs, with CFSE-labeled PBMCs that were stimulated with a pool of γ-irradiated allogeneic PBMCs and cocultured with γ-irradiated BM-MDSCs. After 7 days, cell cultures were harvested, and CD3ζ chain expression was determined by intracellular staining after gating on $CFSE^+CD8^+CD3\epsilon^+$ cells. As shown in the representative experiment of Figure 1A, BM-MDSCs induced a marked decrease in T-lymphocyte proliferation, and this effect was accompanied by a significant reduction in the intracellular levels of CD3ζ chain in $CD8^+$ T cells cocultured with BM-MDSCs (Figure 1B); this result was also confirmed by gating on $CFSE^+CD8^+$ T cells (data not shown). Moreover the reduction of CD3ζ chain expression was also accompanied by a decrease in the surface expression of CD3ϵ chain (supplemental Figure 1A), implying that both chains might be the target of BM-MDSC activity; however, down-regulation of CD3ϵ chain expression was less evident in comparison to CD3ζ chain.

Several studies have shown that MDSCs inhibit immune responses through cell-to-cell contact;[6,7] to address this point, we set up cultures with CFSE-labeled PBMCs, which were stimulated with anti-CD3/CD28 and coincubated with BM-MDSCs, either in the presence or absence of a transwell. The insert ensures the flow of metabolites between the 2 chambers, so that if the immune suppression of BM-MDSCs depends exclusively on the release of soluble molecules, the separation would not prevent the suppressive program of BM-MDSCs. As assessed by the reduction of the CFSE dilutions in PBMCs stimulated in the presence of BM-MDSCs compared with the control cultures without BM-MDSCs, an inhibitory effect was evident only in the presence of a cell-to-cell contact between lymphocytes and BM-MDSCs, because separation of BM-MDSCs by the insert did not affect T-cell proliferation (Figure 1C).

We also performed allogeneic MLRs in which the levels of suppression were evaluated through ^{3}HTdR incorporation. MLRs were set up with different combinations of responder and stimulator PBMCs. In these experiments the proliferative rate of responder PBMCs varied, most probably as a result of the different HLA mismatches between effectors and stimulators, which influenced the magnitude of allogeneic response. Interestingly, we observed that in the presence of a high proliferation rate of responder PBMCs ($> 30 \times 10^3$ cpm), BM-MDSCs could exert a significantly higher suppression of the proliferation, in comparison to a lower proliferation rate of responder lymphocytes (Figure 1D). Indeed, when we evaluated the ability of BM-MDSCs to suppress CD3/CD28-mediated T-lymphocyte activation, that is, a condition in which T lymphocytes are massively activated, suppression was achieved in > 90% of the cases, that is, in a higher proportion of cases compared with alloantigen-specific MLRs (data not shown). These results suggest that MDSCs become fully competent in their suppressive function only in the presence of strongly activated T lymphocytes.

Lin^- fraction of BM-MDSCs is responsible for the immune suppressive activity

As described earlier, the gradual increase of CD11b and CD16 expression is used to distinguish among all the differentiation stages of myeloid commitment. CD16 is considered a marker for mature myeloid cells; thus, the $CD11b^+/CD16^-$ cell subset represents a more immature myeloid population than the $CD11b^+/$

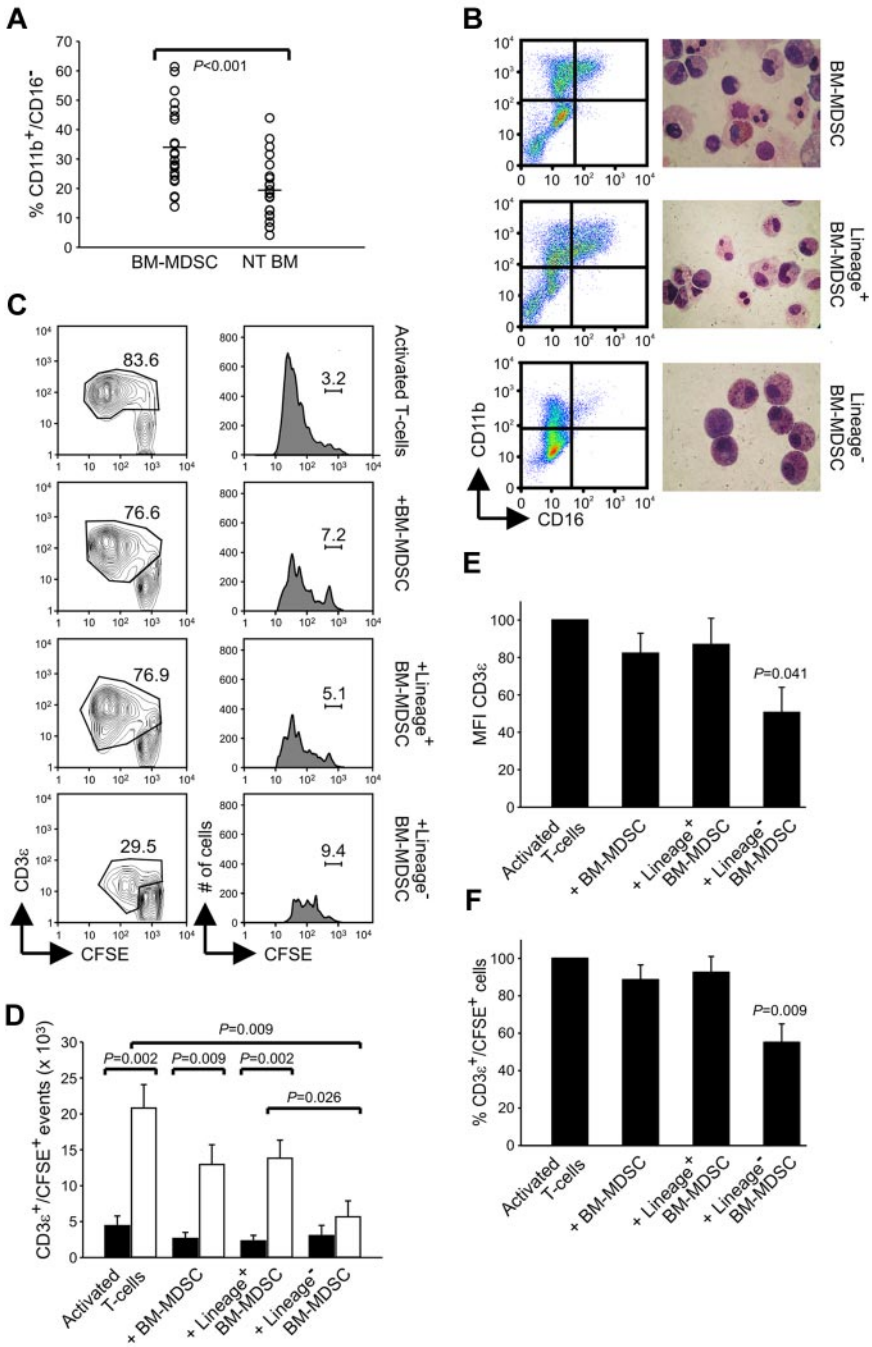

Figure 2. Lin⁻ subset contained within BM-MDSCs shows potent suppressive activity. (A) Flow cytometric analysis of BM cells cultured for 4 days with G-CSF + GM-CSF (BM-MDSCs) or without growth factors (NT BM). At the end of the culture, cells were harvested and labeled, and the percentages of $CD11b^+/CD16^-$ cells were calculated. The figure represents 22 independent experiments; $P \leq .001$, Student *t* test. (B) Flow cytometric profile of CD16 and CD11b expression and May-Grünwald-Giemsa staining on BM-MDSCs before and after immunomagnetic depletion with Lin Ab cocktail. (C) Flow cytometric analysis of the proliferation of allogenic PBMCs, stained with CFSE and activated with anti-CD3 and anti-CD28 for 4 days, in the presence of either BM-MDSCs or the fractions Lin^+ or Lin^- sorted from BM-MDSCs. The figure, in which the percentages of undivided $CD3\epsilon^+/CFSE^+$ lymphocytes are shown, represents 1 of 3 independent experiments. (D) Number of $CD3\epsilon^+/CFSE^+$ events obtained after activation of PBMCs with anti-CD3/CD28 and cocultured in the presence of BM-MDSCs or the subsets Lin^+ and Lin^- sorted from BM-MDSCs. The figure, in which the black bars refer to undivided cells and the gray bars to divided cells, represent the mean ± SE of 6 independent experiments. The values of *P* are indicated in the figure, Mann-Whitney *U* test. (E-F) Evaluation of MFI of CD3ε chain expression and percentage of the $CD3\epsilon^+/CFSE^+$ cells in PBMCs stimulated with anti-CD3/CD28 in the presence of BM-MDSCs or the Lin^+ and Lin^- fractions. Values are mean ± SE of 6 independent experiments. All comparisons among BM-MDSCs containing cultures versus cultures without BM-MDSCs, $P = .041$ (E) and $P = .009$ (F), respectively, Mann-Whitney *U* test.

$CD16^+$ cell subset.[8] We observed that the in vitro expansion of BM-MDSCs with the combination of G-CSF + GM-CSF gave rise to a significant increase in immature $CD11b^+/CD16^-$ elements (Figure 2A; $P < .001$ compared with untreated BM) and that the presence of these cells was correlated with induction of suppressive activity (data not shown).

Interestingly, other groups previously described in patients with cancer an expansion of Lin^- population endowed with suppressive activity.[9] We thus decided to explore the function of more immature subsets among BM-MDSCs after cell enrichment by immunomagnetic sorting with a cocktail of Abs targeting Lin Ags, with the aim to deplete mature myeloid populations and B, T, and natural killer lymphocytes from BM-MDSC cultures. This negative-selection procedure yields a population of cells enriched in hematopoietic stem cells and very early myeloid progenitors that are $CD11b^{low/-}/CD16^-$ (Figure 2B). Although the cell purity is rather high in the Lin^- fraction, the Lin^+ fraction was heterogeneous and still contained lymphocytes, mature, and immature myeloid cells. The structure of the different populations was examined by May-Grünwald-Giemsa staining of cytospin cell preparations and confirmed that unsorted BM-MDSCs were composed of both mononuclear and polymorphonuclear cells, whereas the Lin^- fraction was mainly composed of large mononuclear cells (Figure 2B).

To test the suppressive activity of BM-MDSC fractions we measured the proliferation of T cells (allogeneic with respect to BM-MDSCs) by CFSE dilution after CD3/CD28 stimulation in the presence of unsorted, Lin^-, or Lin^+ BM-MDSC cell subsets. In cultures of T cells stimulated with anti-CD3/CD28, the addition of whole BM-MDSCs caused both a moderate increase in undivided T-cell fraction and a strong reduction in the numbers of $CFSE^+$

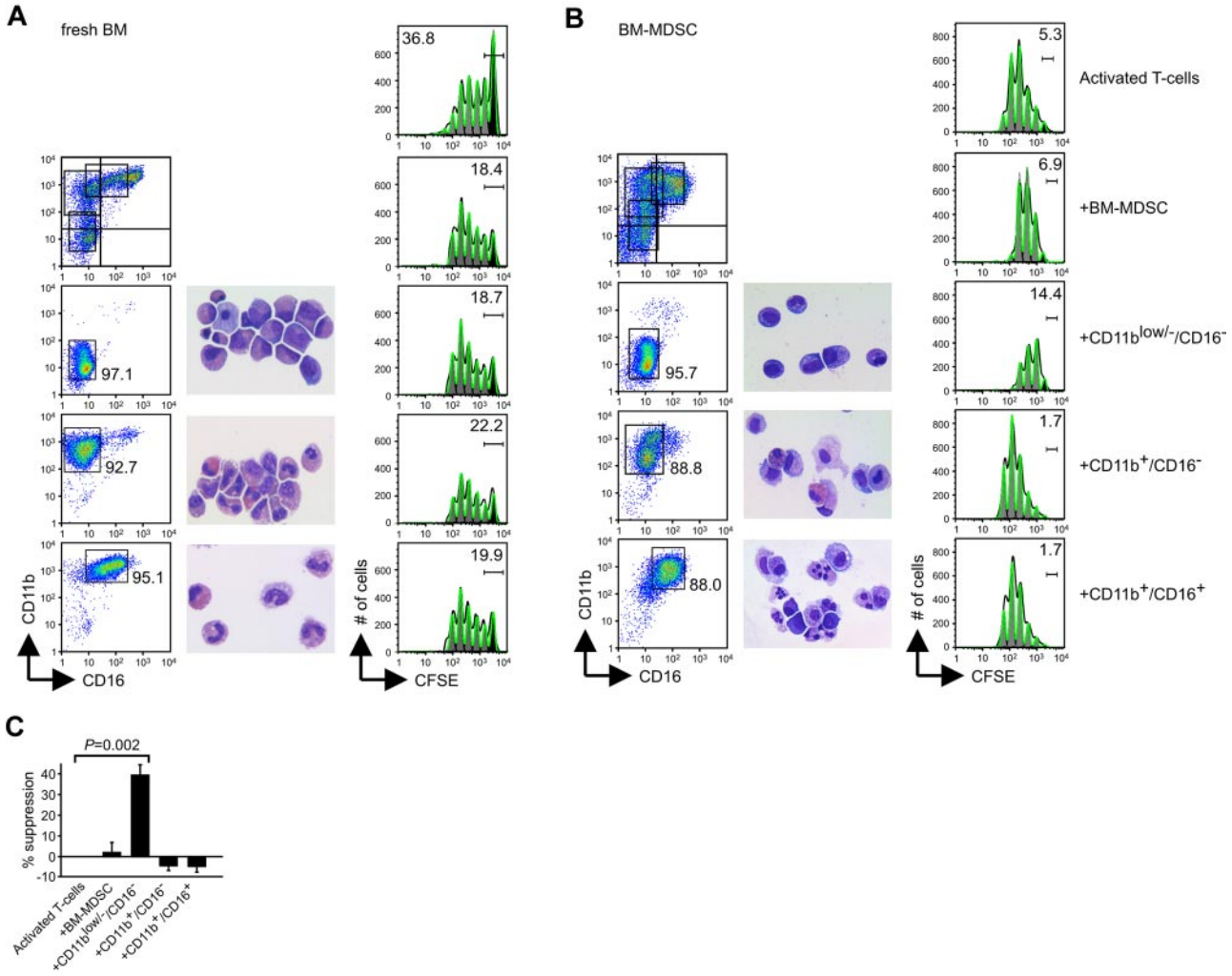

Figure 3. CD11b$^{low/-}$/CD16$^-$ phenotype defines the subset responsible for the immune suppression in BM-MDSCs. (A) Flow cytometric evaluation of CD11b and CD16 markers in BM-MDSC or sorted CD11b$^{low/-}$/CD16$^-$, CD11b$^+$/CD16$^-$ and CD11b$^+$/CD16$^+$ cell populations from fresh BM samples (left), structural analysis by May-Grünwald-Giemsa staining (center), and CFSE dilution proliferation assay (right) in which values reported on histograms represent the percentages of cells in the parental, undivided generation. (B) Flow cytometric evaluation of CD11b and CD16 markers in BM-MDSCs or sorted CD11b$^{low/-}$/CD16$^-$, CD11b$^+$/CD16$^-$, and CD11b$^+$/CD16$^+$ cell populations from BM-MDSCs (left), structural analysis by May-Grünwald-Giemsa staining (center), and CFSE dilution proliferation assay (right) in which values reported on histograms represent the percentages of cells in the parental, undivided generation. (C) Suppression of allogenic CFSE$^+$ PBMCs activated with anti-CD3 and anti-CD28 and cocultured in the presence of 1:1 ratio of the different populations sorted from human BM-MDSCs. The suppression was calculated, analyzing the number of proliferating cells from generation 3 to generation 10, assumed to be 100% without BM-MDSCs. Mean ± SE of 3 independent experiments. $P \leq .01$, Student *t* test, all comparisons among BM-MDSCs containing cultures versus cultures without BM-MDSCs.

cells (Figure 2C-D). The Lin$^-$ fraction was endowed with the highest suppressive activity compared with both the unsorted population and the Lin$^+$ subset, which basically had the same suppressive ability of the unsorted BM-MDSCs (Figure 2C-D).

We also observed that levels of CD3ϵ chain expression in activated T cells suppressed by the Lin$^-$ subset of BM-MDSCs were constantly reduced in terms of MFI (Figure 2E) in all the experiments performed. This decrease in CD3ϵ expression was also accompanied by a significant reduction in the percentage of CD3ϵ$^+$/CFSE$^+$ cells (Figure 2F), therefore suggesting that suppression by the Lin$^-$ subset of myeloid cells was mediated through a profound alteration of signaling machinery associated with a significant reduction in the numbers of CD3$^+$ T lymphocytes.

Suppressive activity of BM-MDSCs is entirely contained within the CD11b$^{low/-}$/CD16$^-$ cell subset

Experiments performed with the Lin$^-$ subset of BM-MDSCs highlighted that cells with the strongest suppressive activity were present in this fraction, supporting data from other laboratories showing that MDSCs obtained from patients with cancer can be traced among Lin$^-$ cells.[9] However, this separation protocol does not allow to distinguish various differentiation stages during myeloid commitment. Therefore, to find out whether suppressive activity of BM-MDSCs was either shared by a number of immature subsets or limited to a specific differentiation stage, we separated defined myeloid subsets through cell sorting.

We sorted 3 different myeloid fractions from fresh BM and cultured BM-MDSCs, based on the expression levels of CD11b and CD16 Ags: the low/negative fraction CD11b$^{low/-}$/CD16$^-$, the intermediate subset CD11b$^+$/CD16$^-$, and the double-positive fraction CD11b$^+$/CD16$^+$, as shown in Figure 3. Because BM-MDSCs do not contain mature granulocytes (CD11b$^+$/CD16^{high}), which are instead present in BM cells, we excluded from the analysis the mature granulocyte population (Figure 3A-B).

May-Grünwald-Giemsa staining showed that both unsorted fresh BM cells and cultured BM-MDSCs had an heterogeneous

structure, as confirmed by other phenotypical features; moreover, in our cell cultures we never found contaminating $CD14^+/CD15^-$ macrophages that could contribute to suppressive activity of BM-MDSCs (data not shown). The $CD11b^{low/-}/CD16^-$ subset isolated from fresh BM cells comprised cell elements with the appearance of myeloid progenitors and promyelocytes, whereas the corresponding subset isolated from BM-MDSCs contained basophilic cells, resembling promyelocytes (Figure 3A-B). The $CD11b^+/CD16^-$ subset separated from fresh BM contained myelocytes, metamyelocytes, eosinophils, and monocytes, whereas BM-MDSCs included mainly cells resembling monocytes and eosinophils. At last, metamyelocytes and band cells were present among $CD11b^+/CD16^+$ cells isolated from both populations.

When we tested the potential suppressive activity of the sorted subsets, only the $CD11b^{low/-}/CD16^-$ cell population isolated from BM-MDSCs was able to suppress the proliferation of activated T cells, whereas the $CD11b^+/CD16^-$ and $CD11b^+/CD16^+$ cell subsets purified from BM-MDSCs were completely devoid of suppressive activity (Figure 3C). Cumulative data reported in Figure 3C show that the entire suppressive activity of BM-MDSCs is contained within a single subset of cytokine-conditioned promyelocytes, which were able not only to block lymphocyte proliferation but also to affect IFN-γ production and to induce T-cell apoptosis (data not shown). None of the 3 corresponding subsets isolated from fresh BM cells was able to interfere with T-lymphocyte proliferation (Figure 3A), further highlighting that priming of BM cells with cytokines is mandatory to induce immunoregulatory MDSCs.

Cytokine-stimulated $CD11b^{low/-}/CD16^-$ cell subset consists of immature and large mononuclear myeloid cells

The phenotype of the suppressive $CD11b^{low/-}/CD16^-$ cell subset was further analyzed by flow cytometry. In the course of our attempt to increase the purity and to minimize the manipulation of sorted cells, we observed that the suppressive $CD11b^{low/-}/CD16^-$ subset could be also separated through a progressive sorting with magnetic beads in which BM-MDSCs were first depleted of $CD3^+$, $CD19^+$, and $CD56^+$ cells, and the resulting population was then depleted of $CD11b^+$ cells. The remaining, negatively selected cell population ($CD11b^{low/-}$ BM-MDSCs) had the same phenotypic and suppressive characteristics of the sorted $CD11b^{low/-}/CD16^-$ BM-MDSCs (supplemental Figure 1B).

$CD11b^{low/-}/CD16^-$ cells sorted from fresh BM had a peculiar structure, characterized by a high side scatter, occupying the region of normal granulocytes, but, after 4 days of culture with G-CSF + GM-CSF, these cells gradually reduced their side scatter and increased the forward scatter, thus moving to the monocyte region (supplemental Figure 1C; Figure 4). However, the surface phenotype of the suppressive $CD11b^{low/-}/CD16^-$ cells, separated from BM-MDSCs, indicated that this population lacked the expression of the monocytic marker CD14 and was positive for the CD15 granulocytic Ag (Figure 4A), thus implying that it had characteristics distinct from both mature monocytes and granulocytes.

The suppressive subset was negative for the lineage markers and expressed the myeloid markers CD13 and CD33; IL4Rα chain was expressed at low intensity, as previously shown.[4,10] The expression of CD66b was down-regulated in the cytokine-treated subset, compared with the same population sorted from fresh BM cells, whereas CD117 increased its expression after induction with G-CSF + GM-CSF (Figure 4A; supplemental Figure 1C). Two discrete populations with different expression of HLA-DR molecule (low or negative) were noted. The suppressive cells expressed CD39 but lacked CD73, which are both expressed on the surface of human T-regulatory lymphocytes.[11] Finally, this subset did not express B7-H1 and slightly expressed B7-H2 and B7-H3 (Figure 4A), members of B7 family that are able to regulate immune responses and to induce immunologic tolerance.[12]

We also estimated the proliferative rate of the $CD11b^{low/-}/CD16^-$ cells by intracellular staining of $Ki\text{-}67^+$ cells and observed that 97% of the cells expressed this Ag, indicating that these cells were actively proliferating in response to cytokine treatment (Figure 4A).

It is known that during the differentiation of polymorphonuclear leukocytes, myeloblasts and promyelocytes proliferate and generate primary granules,[13] and one of the proteins contained in these granules is the enzyme myeloperoxidase (MPO). $CD11b^{low/-}/CD16^-$ cells isolated from BM-MDSCs induced from different human samples could assume either 1 of 2 main structural patterns: cells with large nuclei and reduced cytoplasm without granules and cells with more abundant cytoplasm and a discrete number of cytoplasmic granules (Figure 4B). By confocal microscopy, the MPO protein appeared prevalently located, as expected, within granules; however, the cytoplasm of the agranular cells showed a diffuse pattern of expression (Figure 4B). Classic, mature granulocytes presented the typical polylobated nucleus surrounded by azurophilic granules containing MPO, whereas the MPO expression in monocytes seemed to be confined within the lysosomal compartment (Figure 4B), as described.[14]

We also used a novel monoclonal Ab against human arginase 1 (ARG1) to evaluate whether the enzyme was present in $CD11b^{low/-}/CD16^-$ cells and whether it was coexpressed with MPO, as suggested by some studies.[15] The analysis of ARG1 in this suppressive subset showed cells with different expression pattern: in most cells this enzyme was partially colocalized with MPO, but some cells stained negative for ARG1 (Figure 4B). In contrast, mature granulocytes showed a complete colocalization of the 2 enzymes, whereas monocytes did not express ARG1, as already described.[15] The $CD11b^{low/-}/CD16^-$ cells isolated from fresh BM cells stained positive for ARG1 but showed a decrease of MPO expression, compared with the same population separated from BM-MDSCs (Figure 4C). In comparison, freshly isolated $CD11b^+/CD16^-$ and $CD11b^+/CD16^+$ cells, which represent more advanced maturation stages, presented a progressive increase in the signals for both enzymes (Figure 4C).

Activated T lymphocytes sustain the proliferative rate of the BM-MDSC $CD11b^{low/-}$ cells and block their differentiation process

The activation level of T lymphocytes appears to be critical to drive the suppressive activity of BM-MDSCs (Figure 1D). To investigate the relationship between T-cell activation and MDSC suppression, we set up experiments in which either resting or activated T cells, labeled with CellTrace fluorescent stain, were cocultured with BM-MDSC cell subsets, so that we could trace unambiguously the myeloid and lymphoid cell populations in the coculture and evaluate proliferation after 4 days. As expected, we observed a high proliferation rate of activated T cells in the presence of $CD11b^+$ BM-MDSCs, evaluated in terms of CellTrace dilution and, instead, a reduction in the proliferation of T cells cocultured with the suppressive $CD11b^{low/-}$ BM-MDSC fraction (Figure 5A second lane). We also assessed the cell proliferation of the myeloid cell subsets in the cultures by analyzing Ki-67 expression on gated $CD3^-/CellTrace^-$ cells. Interestingly, although the $CD11b^+$ cell subset of BM-MDSCs did not proliferate in culture with either activated or resting T cells (Figure 5A third lane), the suppressive

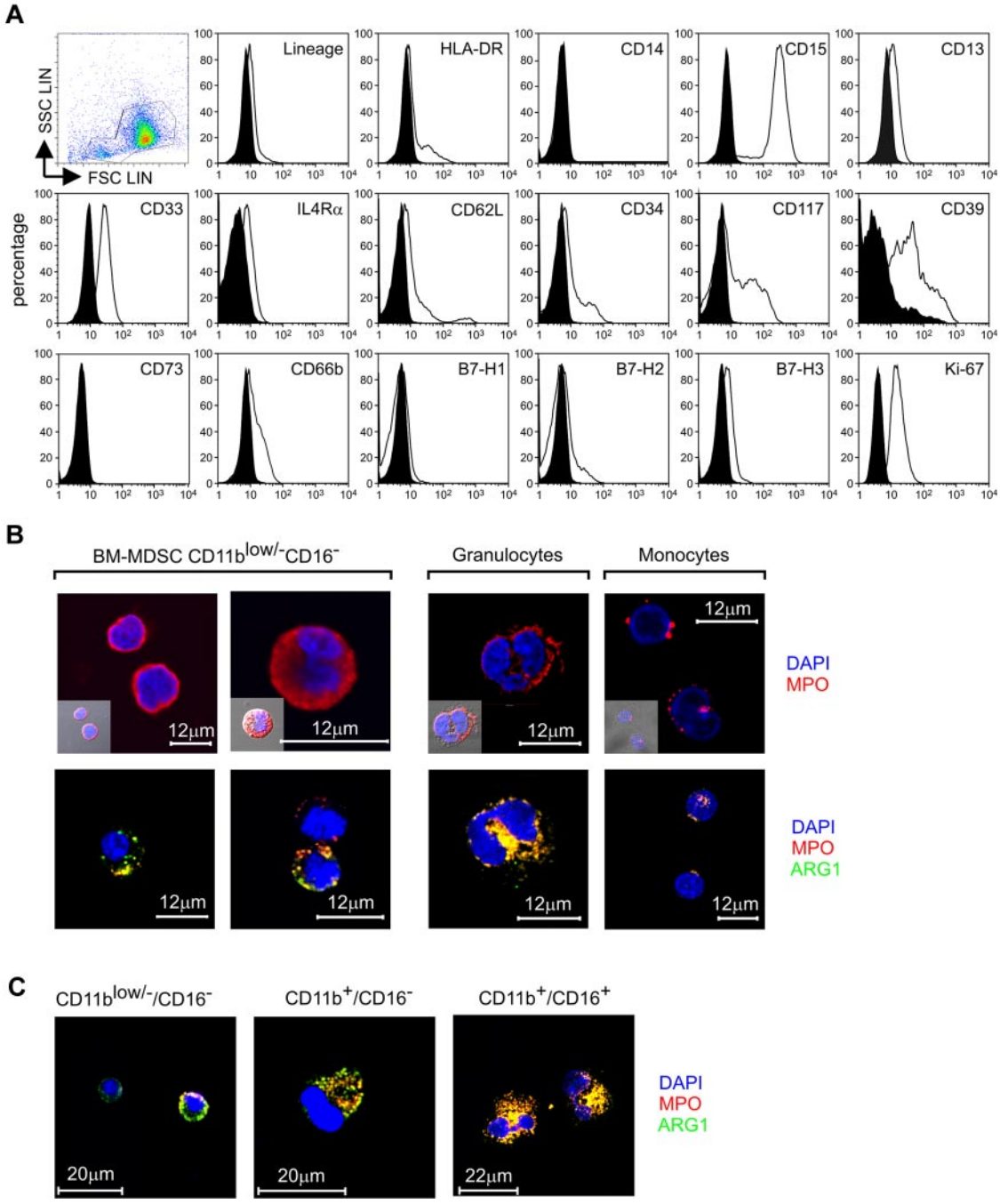

Figure 4. Phenotypic evaluation of the immune-suppressive subset CD11b$^{low/-}$/CD16$^-$ contained within BM-MDSCs. (A) Flow cytometric analysis of CD11b$^{low/-}$/CD16$^-$ cells sorted from BM-MDSCs. The expression of putative MDSCs markers, markers of mature and immature myeloid cells, and markers associated with tolerance was evaluated relative to isotype control (black histograms). In the figure is presented 1 representative of 2 independent experiments. (B) Confocal microscopic localization of MPO and ARG1 in CD11b$^{low/-}$/CD16$^-$ cells, freshly isolated neutrophils, and monocytes. Scale bars = 12 μm. (C) Localization of MPO and ARG1 in CD11b$^{low/-}$/CD16$^-$, CD11b$^+$/CD16$^-$, and CD11b$^+$/CD16$^+$ cells isolated from fresh BM samples determined by confocal microscopy. Scale bars = 20 μm.

CD11b$^{low/-}$ cell subset maintained a discrete proliferative capacity in the presence of resting T cells, which was even increased with the presence of activated T cells (geometric mean fluorescent intensity 14.5 vs 29.2, respectively), suggesting that T-cell activation supports the proliferation of suppressive cells.

To understand whether suppressive BM-MDSC CD11b$^{low/-}$ cells maintain their phenotype or rather differentiate to more mature myeloid subsets when cocultured with activated T lymphocytes, we analyzed the expression of differentiation myeloid markers after cell coculture. After 4 days of culture we observed that, only in the presence of activated T cells, promyelocyte-like cells maintained their level of immaturity, as shown by the levels of expression in the markers CD11b and CD16; moreover, whereas HLA-DR and CD34 were maintained or even increased, CD66b, a marker of secondary granules, was downregulated in the presence of activated T cells (Figure 5B). Control cultures of immature promelocyte-like cells in the absence of lymphocytes showed a differentiation pattern similar to myeloid cells cocultured with resting T cells (Figure 5B), thus suggesting that only the presence of activated T cells is able to block the default differentiation process of immature promyelocyte-like cells.

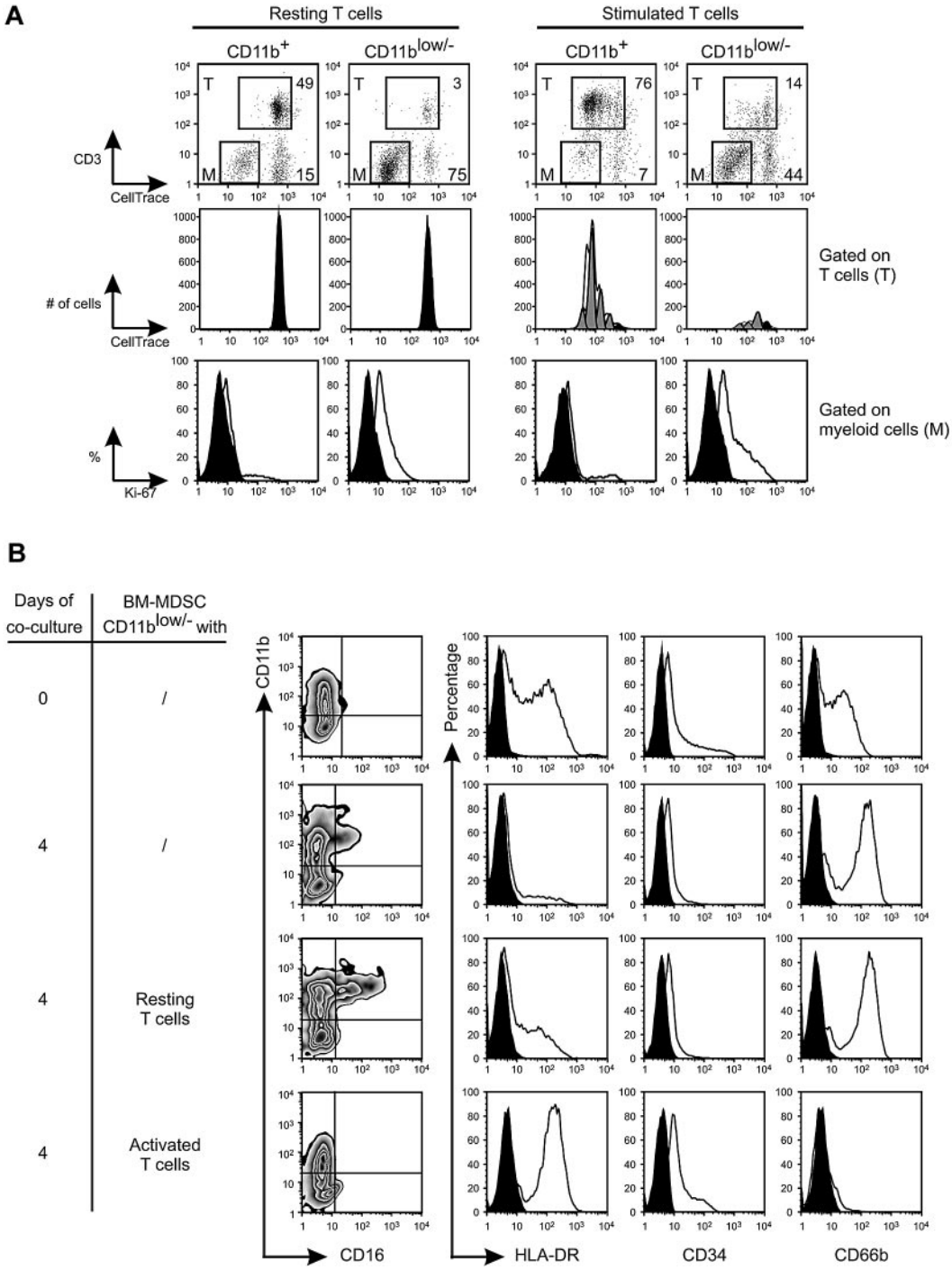

Figure 5. T-lymphocyte activation is driving BM-MDSC proliferation and immune suppression. (A) CellTrace-labeled PBMCs were stimulated with anti-CD3/CD28 in the presence of BM-MDSC CD11b^{+} and CD11b$^{low/-}$ cell subsets, added at a ratio of 1:1. After 3 days, cell cultures were harvested, labeled with anti-CD3ε, and analyzed in the CD3ε^{-}/CellTrace^{-} gate (M) and in the CD3ε^{+}/CellTrace^{+} (T) cell gate. The numbers indicated in the top graphs refer to the percentage of cells gated on either T cells (T) or on myeloid cells (M). The central histograms show the profile of CellTrace dilution of either resting or stimulated T cells (gate T) cocultured with BM-MDSCs CD11b^{+} and CD11b$^{low/-}$ subsets. Black and gray curves refer to undivided and proliferating cells, respectively. The bottom histograms show Ki-67 expression in BM-MDSCs CD11b^{+} and CD11b$^{low/-}$ subsets (gate M) cocultured with either resting or stimulated T cells. Black histograms indicate isotype control. The figure shows a representative experiment of 3 performed. (B) Flow cytometric evaluation of CD11b, CD16, HLA-DR, CD34, and CD66b markers in CD11b$^{low/-}$ cell subset sorted from BM-MDSCs either before or after the coculture with resting or anti-CD3/anti-CD28–activated T cells. The expression of these markers was compared with the autofluorescence signal (black histograms). In the figure, 1 representative of 3 independent experiments is presented.

Taken together these data indicate that promyelocyte-like cells proliferate, their functional activity is associated with a delay in the differentiation pathway, and both proliferation and block in the differentiation pathway account for their expansion and maintenance of an immature phenotype.

Increased circulating MDSC levels correlate with progression and worse clinical prognosis

The suppressive myeloid population of BM-MDSCs was mainly Lin^{-}, CD11b$^{low/-}$, HLA-DR$^{low/-}$, but positive for myeloid markers

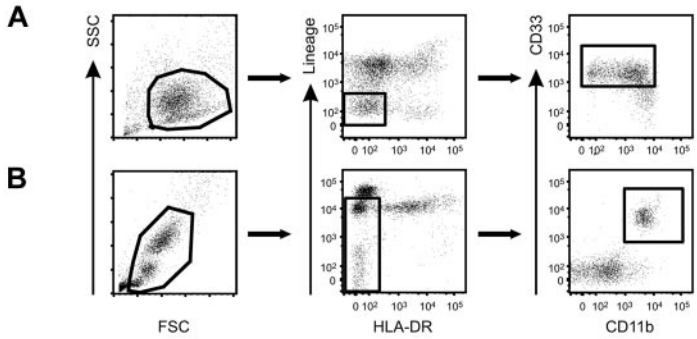

C

Independent Variable	Dependent Variable	Coefficient (95% CI)	P-Value	Pearson Correlation
% MDSC	CTC	0.29 (0.14, 0.43)	0.0001	0.62
% MDSC	Swenerton Score	0.28 (-0.76, 0.64)	0.12	0.31
CTC	Swenerton Score	0.43 (-0.82, 0.91)	0.92	0.0049

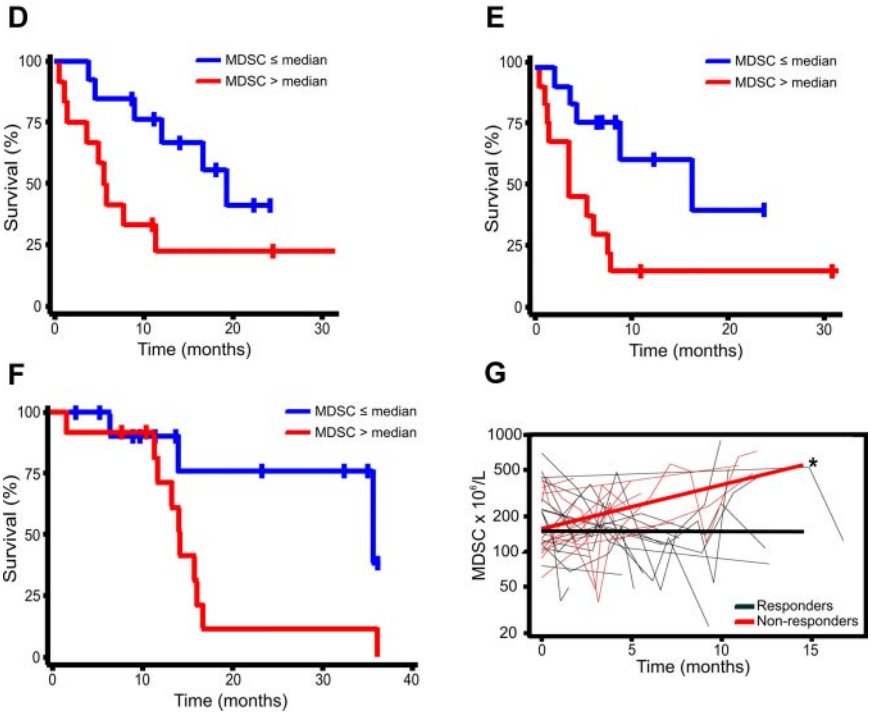

Figure 6. Increase in circulating MDSC levels over time in patients with advanced solid tumors is associated with decreased survival times and radiographic disease progression. Gating strategy for BM-MDSCs (A) and whole-blood MDSCs (B) is shown on a representative flow cytometric plot. (C) Random effects regression model and correlation between MDSCs and CTCs. Flow cytometric analysis was performed on peripheral whole blood in a separate cohort of patients with stage IV breast cancer (n = 25) before initiation of therapy and at defined intervals during therapy. Blood for CTC determination by the CellSearch was simultaneously drawn. A significant correlation was found between circulating MDSC levels (%) and CTCs ($P = .0001$). (D) Survival analysis by circulating MDSC levels (%) at first blood draw in patients with stage IV breast cancer starting a new line of systemic chemotherapy (n = 26). Survival estimates by median percentage of MDSCs (≤ 3.17% and > 3.17%) with the use of the first MDSCs observation ($P = .048$). (E) Survival estimates by median percentage of MDSCs (≤ 3.04% and > 3.04%) with the use of MDSCs levels drawn at the last visit ($P = .018$). (F) Survival analysis by circulating MDSC levels at time of study enrollment in patients with stage IV colorectal cancer. Survival estimates by medial percentage of MDSCs (≤ 2.54% and > 2.54%). (G) Analysis of relationship between changes in circulating MDSC levels over time and best radiographic response in patients receiving systemic chemotherapy (n = 25). Plot of MDSCs over time by "best response" defined as patients who achieved complete (CR) or partial radiographic response (PR) while on systemic therapy versus patients who did not. MDSCs were drawn prospectively after every other cycle of therapy. Over time circulating MDSCs were significantly higher in nonresponders than in patients with CR or PR as best response (*$P = .015$ comparing slopes).

CD33 (Figure 4), a subset with phenotype similar to MDSCs previously described in tumor-bearing patients.[9,16] Indeed, in the blood of patients with stage IV breast cancer we could clearly identify a Lin$^-$, HLA-DR$^-$, CD33$^+$, CD11b$^+$ MDSC population resembling in vitro–generated BM-MDSCs (Figure 6A-B). We previously showed that this cell subset correlated with clinical tumor stage,[16] but it is still unknown whether circulating Lin$^-$, HLA-DR$^-$, CD33$^+$, CD11b$^+$ cells also correlate with either metastatic tumor burden or OS in patients with cancer. We thus evaluated the relationship between MDSCs and CTCs measured by the CellSearch assay, a strong, independent predictor of survival in patients with advanced breast cancer.[17,18] In a cohort of patients with stage IV breast cancer (n = 25) CTCs (CellSearch) and MDSCs were analyzed simultaneously. A generalized estimating equation regression model was created and fitted individually for each predictor. A significant correlation was observed between

circulating MDSCs and CTCs ($P = .0001$; Figure 6C). As expected, no significant correlation was observed between CTCs and SS ($P = .92$); indeed, CTCs are not a measure of metastatic tumor burden, and levels do not correlate with SS in patients with advanced breast cancer.[17-19] To ascertain whether high circulating MDSC levels were associated with poorer prognosis, survival estimates in the breast cancer dataset were calculated with MDSC levels (%), drawn either before starting a new line of therapy or levels at the last blood draw. Patients with circulating MDSCs $> 3.17\%$ (median) at baseline had a poorer OS than patients with circulating MDSCs $\leq 3.17\%$, with median OS times of 5.5 months (95% confidence interval [CI], 0.5-11.3 months) and 19.32 months (95% CI, 8.7 months to infinity), respectively ($P = .048$; Figure 6D). Likewise, elevated MDSC levels at the last visit were also associated with a significantly poorer OS ($P = .018$), with median survival times of 3.8 months (95% CI, 0.5-7.7 months) and 16.7 months (95% CI, 3.8 months to infinity), respectively (Figure 6E).

We then moved to examine another group of patients with cancer. In a cohort of patients with stage IV colorectal cancer ($n = 25$) we also found that baseline levels of MDSCs before starting chemotherapy also correlated with poorer OS (Figure 6F). Patients with circulating MDSC levels greater than the median value (2.54%) had significantly shorter median OS times than patients with levels below the median value (35.6 vs 14.3 months; $P = .025$; Figure 6F). We next investigated whether levels of circulating MDSCs over time in patients with advanced solid tumors receiving systemic chemotherapy correlated with clinical outcomes. MDSC levels in the same cohort of patients with stage IV colorectal cancer were drawn every other chemotherapy cycle. Patients underwent routine radiographic assessments as clinically indicated, typically every 2-3 months. Over time MDSC levels were significantly higher in patients who had radiographic evidence of progressive disease than in levels in patients who achieved either a CR or PR as their best radiographic response ($P = .015$; Figure 6G). Taken together, these clinical data suggest, for the first time, that circulating MDSC levels, phenotypically similar to those described in human BM experiments, are clinically relevant and appear to (1) increase over time in patients with progressive disease, (2) correlate with an established prognostic marker (CTCs) in advanced breast cancer, and (3) show that persistently high or increasing levels after chemotherapy are associated with poorer survival.

Discussion

The aim of our study was to dissect the differentiation stage of the suppressive myeloid cells by taking advantage of the in vitro generation of MDSCs from the BM precursor.[3] The suppressive activity is fully induced in BM-MDSCs only after direct contact with activated T lymphocytes, indicating that suppressive cells are primed by the activation status of target cells and by a cell membrane signal, a result analogous to data obtained with mouse MDSCs.[10] Moreover, this result is in line with the consideration that myeloid suppressors play a role in turning off potential harmful immune responses carried out by activated T lymphocytes.[1,20] Our results extend this idea, leading us to hypothesize that the activity of MDSCs is dictated by the activation level of the T lymphocytes. In fact, suppressive cells are unable to harm resting lymphocytes, and the direct contact between these 2 cells might ensure that the signals delivered by MDSCs are confined only to target cells and not to bystander cells.

It is known that anti-CD3– and anti-CD28–activated T cells secrete GM-CSF and IL-6,[21] cytokines that drive the BM-MDSC development from BM; however, we observed that BM-MDSCs also are able to produce in vitro IL-6 during the culture with growth factors (data not shown). Moreover, it was recently shown that T lymphocytes, on TCR activation, produce soluble factors that enhance fibroblasts production of IL-6.[22] An attractive hypothesis is that activated T cells release cytokines that might sustain the induction of the suppressive cells or maintain their tolerogenic activity, an autoregulative loop that has already been shown in a different system.[10]

Among different cytokine combinations, GM-CSF and IL-6 were the most effective in generating, from healthy donor PBMCs, suppressive $CD33^+$ cells that inhibited the proliferation and IFN-γ production by autologous human T cells after CD3/CD28 stimulation.[23] These cells were large mononuclear $CD11b^+$ $HLA\text{-}DR^{low}$ $CD66b^+$ cells with basophilic and granular cytoplasm. When molecules and enzymes participating in inhibitory pathways were evaluated by either quantitative RT-PCR or cytofluorometry, NOS2, TGFβ, VEGF, and NOX2 were found to be up-regulated, whereas no significant changes in comparison with the nonsuppressive, normal $CD33^+$ cells were detected for B7-H1, B7-H2, and B7-H4.[23] It thus appears that cytokines might induce different cells with immunoregulatory properties when acting on either BM or blood-circulating precursors. Whether these cells represent stages of the same differentiation process is an issue that requires further investigation. It is clear, however, that MDSCs described in the present study are different from either fully differentiated or activated granulocytes and monocytes.

We observed that the reduction of lymphocyte proliferation induced by BM-MDSCs is accompanied by a decreased expression not only of the CD3ζ but also of the CD3ϵ chain and by a reduction in absolute numbers of T lymphocytes. It is known that the absence or reduction of CD3ζ chain impairs T-cell signaling and contributes to immune cell dysfunction and evidence is accumulating that expression of the CD3ζ chain is markedly decreased in both peripheral blood and tumor-infiltrating lymphocytes in patients with different types of tumors.[24,25] Significantly less is known about the importance of the ϵ chain of the CD3/TCR complex in tumor immunity, even if some reports have shown down-regulation of CD3ϵ chain in patients with lung cancer and SCID.[26-28]

In this study we addressed the extent and relevance of cell heterogeneity of MDSCs, generally accepted as a common feature of this cell population, with the aim to define whether immunoregulatory properties of human BM-MDSCs can be attributed to ≥ 1 cell subsets. We observed that the treatment of BM cells with G-CSF + GM-CSF resulted in a significant accumulation of immature myeloid cells (Figure 2A).[3] In this regard, we observed that one of the differences existing between untreated BM and BM-MDSCs was represented by the expansion of immature myeloid cells expressing low levels of CD11b and negative for CD16, a phenotype that is typically associated with myeloblasts and promyelocytes, but not with more differentiated cells (Figure 2A and[3]). The accumulation of immature $CD11b^+/CD16^-$ cells in BM-MDSCs led us to test the hypothesis that this myeloid population was entirely responsible for the suppression exerted by BM-MDSCs. Our results clearly indicate that the only subset responsible for the immune suppression exerted by BM-MDSCs is contained within the $CD11b^{low/-}/CD16^-$ cell population of BM-MDSCs, and other immature but more differentiated subsets, such

as $CD11b^+/CD16^-$ and $CD11b^+/CD16^+$ cells, are completely devoid of suppressive activity; accordingly, this subset was able to proliferate in the presence of activated T cells, a feature that is lost by more mature subsets. Interestingly, we also observed that BM-MDSC $CD11b^{low/-}$ were able to exert suppressive activity both on $CD4^+$ and $CD8^+$ subsets and to induce apoptosis of T cells, an event that was marginal in T cells activated without BM-MDSC $CD11b^{low/-}$ (data not shown).

Remarkably, the suppressive cell subset had a phenotype corresponding to promyelocytes, and, indeed, these cells structurally resembled promyelocytes, with a large regular, symmetric nucleus, high nucleus/cytoplasm ratio, and basophilic cytoplasm. We sorted the corresponding subset from fresh BM ($CD11b^{low/-}/CD16^-$), containing mainly promyelocytes. The 2 subsets were indistinguishable from a structural point of view, but they differed completely in terms of ability to suppress activated T lymphocytes, because normal promyelocytes were unable to exert any inhibitory activity (Figure 3A). Here, for the first time, we show that MDSCs proliferate, that this activity is linked to a block in the differentiation pathway, and, interestingly, that both suppression and maturation depend on the activation status of the T lymphocytes (Figure 5).

Because suppressive activity of myeloid cells is limited to a specific subset of promyelocytic-like cells, and the more differentiated populations are completely devoid of regulatory activity, this implies that suppressive activity is not a stable trait of MDSCs but rather a transitory state, possibly ending or being sustained according to local signals coming from the microenvironment where the immature cells migrate. These results, therefore, suggest that MDSCs maintain a plasticity that enables them to differentiate and suspend their tolerogenic program.

We found that ARG1 was expressed in the suppressive $CD11b^{low/-}/CD16^-$ cell subset and partially colocalized with MPO, suggesting its main distribution within primary granules, as suggested by Munder et al.[15] However, in comparison with the same population isolated from fresh BM, this subset had an increased expression of MPO, which presented both an expected granular and an uncommon agranular localization. We are currently evaluating whether the altered expression of these enzymes is only a marker of these cells or whether it is related also to their suppressive function.

Finally, one of the challenges in studying MDSCs in humans has been that the phenotype is not as well defined as in mice. We show that MDSCs, defined as Lin^-, HLA DR^-, $CD33^+$, $CD11b^+$, can be easily traced among blood circulating cells in patients with advanced breast and patients with colorectal cancer, with levels correlating with clinical outcomes.

Acknowledgments

The authors thank Drs A. Anselmo for help and advice with FACS, C. Frasson for FACS, and P. Gallo for artwork preparation.

This work was supported by grants from the Italian Ministry of Health, Fondazione Cassa di Risparmio di Padova e Rovigo, Italian Association for Cancer Research (AIRC), Association for International Cancer Research (AICR; grant 08-0518), and Fondazione Cassa di Risparmio di Verona, Vicenza, Belluno e Ancona and Associazione Italiana Ricerca sul Cancro (AIRC; grant 6599).

Authorship

Contribution: S.S. performed research, analyzed and interpreted data, and wrote the manuscript; E.F. performed flow cytometry and confocal microscopy studies; C.M.D.-M. performed flow cytometric analysis of all data from patients with solid tumors, analyzed and discussed results; A.D. performed confocal microscopy study; L.P. performed research; A.R. generated monoclonal Ab against ARG1; S.F. performed BM samples enrollment; G.B. discussed results and provided vital material for the study; P.Z. discussed the results; G.O. and E.G.-M. performed statistical analyses of data from patients with breast cancer and with colorectal cancer; A.J.M. obtained informed consent on all patients with solid tumors, helped write results on relevant section, and edited manuscript; V.B. discussed and analyzed the results and wrote the manuscript; and S.M. designed the study, analyzed and interpreted data, and wrote the manuscript.

Conflict-of-interest disclosure: The authors declare no competing financial interests.

The current affiliation for V.B. is Immunology Section, Verona University Hospital and Department of Pathology, Verona, Italy.

Correspondence: Susanna Mandruzzato, Oncology Section, Department of Oncology and Surgical Sciences, Via Gattamelata, 64 35128 Padova, Italy; e-mail: susanna.mandruzzato@unipd.it.

References

1. Gabrilovich DI, Nagaraj S. Myeloid-derived suppressor cells as regulators of the immune system. *Nat Rev Immunol.* 2009;9(3):162-174.
2. Peranzoni E, Zilio S, Marigo I, et al. Myeloid-derived suppressor cell heterogeneity and subset definition. *Curr Opin Immunol.* 2010;22(2):238-244.
3. Marigo I, Bosio E, Solito S, et al. Tumor-induced tolerance and immune suppression depend on the C/EBPbeta transcription factor. *Immunity.* 2010;32(6):790-802.
4. Mandruzzato S, Solito S, Falisi E, et al. IL4Ralpha+ myeloid-derived suppressor cell expansion in cancer patients. *J Immunol.* 2009; 182(10):6562-6568.
5. Rodriguez PC, Ochoa AC. Arginine regulation by myeloid derived suppressor cells and tolerance in cancer: mechanisms and therapeutic perspectives. *Immunol Rev.* 2008;222:180-191.
6. Dugast AS, Haudebourg T, Coulon F, et al. Myeloid-derived suppressor cells accumulate in kidney allograft tolerance and specifically suppress effector T cell expansion. *J Immunol.* 2008; 180(12):7898-7906.
7. Apolloni E, Bronte V, Mazzoni A, et al. Immortalized myeloid suppressor cells trigger apoptosis in antigen-activated T lymphocytes. *J Immunol.* 2000;165(12):6723-6730.
8. Elghetany MT, Ge Y, Patel J, Martinez J, Uhrova H. Flow cytometric study of neutrophilic granulopoiesis in normal bone marrow using an expanded panel of antibodies: correlation with morphologic assessments. *J Clin Lab Anal.* 2004; 18(1):36-41.
9. Almand B, Clark JI, Nikitina E, et al. Increased production of immature myeloid cells in cancer patients: a mechanism of immunosuppression in cancer. *J Immunol.* 2001;166(1):678-689.
10. Gallina G, Dolcetti L, Serafini P, et al. Tumors induce a subset of inflammatory monocytes with immunosuppressive activity on CD8+ T cells. *J Clin Invest.* 2006;116(10):2777-2790.
11. Deaglio S, Dwyer KM, Gao W, et al. Adenosine generation catalyzed by CD39 and CD73 expressed on regulatory T cells mediates immune suppression. *J Exp Med.* 2007;204(6):1257-1265.
12. Latchman Y, Wood CR, Chernova T, et al. PD-L2 is a second ligand for PD-1 and inhibits T cell activation. *Nat Immunol.* 2001;2(3):261-268.
13. Borregaard N, Cowland JB. Granules of the human neutrophilic polymorphonuclear leukocyte. *Blood.* 1997;89(10):3503-3521.
14. Bunbury A, Potolicchio I, Maitra R, Santambrogio L. Functional analysis of monocyte MHC class II compartments. *FASEB J.* 2009;23(1):164-171.
15. Munder M, Mollinedo F, Calafat J, et al. Arginase I is constitutively expressed in human granulocytes and participates in fungicidal activity. *Blood.* 2005;105(6):2549-2556.
16. Diaz-Montero CM, Salem ML, Nishimura MI, Garrett-Mayer E, Cole DJ, Montero AJ. Increased circulating myeloid-derived suppressor cells correlate with clinical cancer stage, metastatic tumor burden, and doxorubicin-cyclophosphamide chemotherapy. *Cancer Immunol Immunother.* 2009; 58(1):49-59.

17. Cristofanilli M, Budd GT, Ellis MJ, et al. Circulating tumor cells, disease progression, and survival in metastatic breast cancer. *N Engl J Med.* 2004; 351(8):781-791.

18. Cristofanilli M, Broglio KR, Guarneri V, et al. Circulating tumor cells in metastatic breast cancer: biologic staging beyond tumor burden. *Clin Breast Cancer.* 2007;7(6):471-479.

19. Cristofanilli M, Hayes DF, Budd GT, et al. Circulating tumor cells: a novel prognostic factor for newly diagnosed metastatic breast cancer. *J Clin Oncol.* 2005;23(7):1420-1430.

20. Marigo I, Dolcetti L, Serafini P, Zanovello P, Bronte V. Tumor-induced tolerance and immune suppression by myeloid derived suppressor cells. *Immunol Rev.* 2008;222:162-179.

21. Harris KM, Lenz P, Hankey KG, et al. Products of anti-CD3/anti-CD28 activated lymphocytes induce differentiation and maturation of dendritic cells and have adjuvant-like activity in vitro and in vivo. *Clin Immunol.* 2008;129(1):58-68.

22. Barnas JL, Simpson-Abelson MR, Brooks SP, Kelleher RJ Jr, Bankert RB. Reciprocal functional modulation of the activation of T lymphocytes and fibroblasts derived from human solid tumors. *J Immunol.* 2010;185(5):2681-2692.

23. Lechner MG, Liebertz DJ, Epstein AL. Characterization of cytokine-induced myeloid-derived suppressor cells from normal human peripheral blood mononuclear cells. *J Immunol.* 2010;185(4): 2273-2284.

24. Schule J, Bergkvist L, Hakansson L, Gustafsson B, Hakansson A. Down-regulation of the CD3-zeta chain in sentinel node biopsies from breast cancer patients. *Breast Cancer Res Treat.* 2002;74(1):33-40.

25. Otsuji M, Kimura Y, Aoe T, Okamoto Y, Saito T. Oxidative stress by tumor-derived macrophages suppresses the expression of CD3 zeta chain of T-cell receptor complex and antigen-specific T-cell responses. *Proc Natl Acad Sci U S A.* 1996; 93(23):13119-13124.

26. de Saint Basile G, Geissmann F, Flori E, et al. Severe combined immunodeficiency caused by deficiency in either the delta or the epsilon subunit of CD3. *J Clin Invest.* 2004;114(10):1512-1517.

27. Prado-Garcia H, Aguilar-Cazares D, Meneses-Flores M, Morales-Fuentes J, Lopez-Gonzalez JS. Lung carcinomas do not induce T-cell apoptosis via the Fas/Fas ligand pathway but down-regulate CD3 epsilon expression. *Cancer Immunol Immunother.* 2008;57(3):325-336.

28. Kuang DM, Zhao Q, Xu J, Yun JP, Wu C, Zheng L. Tumor-educated tolerogenic dendritic cells induce CD3epsilon down-regulation and apoptosis of T cells through oxygen-dependent pathways. *J Immunol.* 2008;181(5):3089-3098.